Mon. Not. R. Astron. Soc. **422,** 3130–3141 (2012)

doi:10.1111/j.1365-2966.2012.20834.x

The peculiar 2011 outburst of the black hole candidate IGR J17091−3624, a GRS 1915+105-like source?

F. Capitanio,[1★] M. Del Santo,[1] E. Bozzo,[2] C. Ferrigno,[2] G. De Cesare[1] and A. Paizis[3]

[1] *Istituto Nazionale di Astrofisica, IAPS, Via Fosso del Cavaliere 100, 00133 Rome, Italy*
[2] *ISDC Data Centre for Astrophysics, Chemin d'Ecogia 16, 1290 Versoix, Switzerland*
[3] *Istituto Nazionale di Astrofisica, IASF-Mi, Via Bassini 15, I-20133 Milano, Italy*

Accepted 2012 February 28. Received 2012 February 24; in original form 2011 October 19

ABSTRACT

We report on the long-term monitoring campaign of the black hole candidate IGR J17091−3624 performed with *INTEGRAL* and *Swift* during the peculiar outburst started on 2011 January. We have studied the two-month spectral evolution of the source in detail. Unlike the previous outbursts, the initial transition from the hard to the soft state in 2011 was not followed by the standard spectral evolution expected for a transient black hole binary. IGR J17091−3624 showed pseudo-periodic flare-like events in the light curve, closely resembling those observed from GRS 1915+105. We find evidence that these phenomena are due to the same physical instability process ascribed to GRS 1915+105. Finally, we speculate that the faintness of IGR J17091−3624 could be not only due to the high distance of the source but also due to the high inclination angle of the system.

Key words: accretion, accretion discs – methods: observational – X-rays: binaries.

1 INTRODUCTION

The black hole candidate (BHC) IGR J17091−3624 was discovered by *INTEGRAL*/IBIS during a Galactic Centre observation on 2003 April 14 and 15 (Kuulkers et al. 2003). At the onset of the discovery outburst, the source showed a hard spectrum with a flux of about ∼20 mCrab in the 40–100 keV energy range. The analysis of IBIS, JEM-X and *RXTE*/PCA data of the whole outburst (Lutovinov & Revnivtsev 2003; Capitanio et al. 2005; Lutovinov et al. 2005) revealed an indication of a hysteresis-like behaviour. The presence of a hot disc blackbody emission component during the softening of the X-ray emission of the source was also unveiled.

After the *INTEGRAL* discovery, IGR J17091−3624 was searched in the archival data of both TTM-KVANT (Revnivtsev et al. 2003) and *BeppoSAX*/Wide Field Camera (WFC; in't Zand et al. 2003). In the former archive, one outburst was discovered dating back to 1994 and reaching a flux of 10 mCrab in the 3–30 keV energy band; the analysis of *BeppoSAX*/WFC data revealed that a second outburst had occurred in 2001, reaching a flux of 14–20 mCrab (2–10 keV).

IGR J17091−3624 lies at 9.6 arcmin from another transient X-ray binary, IGR J17098−3628, discovered on 2005 March 24 (Grebenev, Molkov & Sunyaev 2005) when it underwent a 4-yr-long outburst (Capitanio et al. 2009a). On 2006 August 29 and 2007 February 19, two *XMM–Newton* observations of the region around these two sources were performed. While IGR J17098−3628 was detected in a relatively bright state in both observations, IGR J17091−3624 was not detected and an X-ray upper limit of 7 × 10^{32} erg s^{-1} was obtained (assuming a distance of 8 kpc; Capitanio et al. 2009a).

The refined position of IGR J17091−3624 provided by Kennea & Capitanio (2009) ruled out the tentative radio counterpart previously proposed for the source (Rupen, Mioduszewski & Dhawan 2003; Pandey et al. 2006). A re-analysis of the archival radio observations performed 9 d after the source discovery by IBIS in 2003 enabled the identification of a faint transient radio source (sub-mJy level at 5 GHz) that showed a flux increase in the subsequent two weeks and an inverted spectrum, a signature of a compact jet (Capitanio et al. 2009a). This was consistent with the low/hard spectral state (hereafter LHS) observed by *INTEGRAL* in the same period (Capitanio et al. 2005). The source behaviour during the 2007 observation campaign was typical of a BHC in outburst, even if the relatively low X-ray flux of the source (the 0.5–10 keV peak flux of ∼2 × 10^{-9} erg cm^{-2} s^{-1}) hindered a detailed spectral evolution study (Capitanio et al. 2009a).

At the end of 2011 January, the *Swift*/BAT hard X-ray transient monitor reported a renewed activity from IGR J17091−3624. The source flux increased from 20 mCrab on January 28 up to 60 mCrab on February 3 in the energy range 15–50 keV (Krimm & Kennea 2011; Krimm et al. 2011). The corresponding XRT spectrum obtained with a ToO observation was well described by an absorbed power law with a photon index of 1.73 ± 0.29 (Krimm & Kennea 2011). On 2011 February 7, the region around IGR J17091−3624 was also observed by the IBIS/ISGRI and JEM-X telescopes on-board the *INTEGRAL* satellite. The estimated source flux in the 20–100 keV energy range was 120 mCrab. The

---

★E-mail: fiamma.capitanio@iasf-roma.inaf.it

combined ISGRI+JEM-X spectrum (5–200 keV) could be well described by an absorbed cut-off power-law model with a photon index of ∼1.4 and a high-energy cut-off of about 110 keV. This suggested that the source was in LHS (Capitanio et al. 2011).

Follow-up radio observations carried out with the ATCA telescope measured a flat spectrum (Corbel et al. 2011; Rodriguez et al. 2011b; Torres et al. 2011) associated with self-absorbed compact jets, as expected in accreting black holes (BHs) in the LHS. Later on, Rodriguez et al. (2011b) also reported on the detection of a discrete jet ejection event usually observed when a BHC undergoes a transition from the hard intermediate state (HIMS) to the soft intermediate state (SIMS). A 0.1-Hz QPO, increasing in frequency with the source flux and spectral softening, was revealed by both Rodriguez et al. (2011a) and Shaposhnikov (2011). These findings motivated a long monitoring campaign that was carried out with *Swift*/XRT, starting on February 28. The XRT observations were planned to be simultaneous with the *INTEGRAL* pointings already scheduled in the direction of the source, in order to ensure the broadest possible energy coverage (0.3–200 keV) during the entire outburst.

As reported by Del Santo et al. (2011), on February 28 the XRT+IBIS joint spectrum resulted in a typical high soft state (HSS) shape, with a prominent disc blackbody component ($kT_{\rm in} \sim 1$ keV) and a power-law photon index of 2.2 ± 0.2. No high-energy cut-off was present up to 200 keV. On 2011 March 14 (MJD 55634), a ∼10-mHz QPO was detected in a 3.5-ks *RXTE* observation (Altamirano et al. 2011a). One week later, *RXTE*/PCA showed a continuous progression of quasi-periodic flare-like events occurring at a rate between 25 and 30 mHz. This kind of variability resembles the 'heartbeat' variation observed in the BH binary GRS 1915+105 (Altamirano et al. 2011b; Pahari, Yadav & Bhattacharyya 2011a,b). Altamirano et al. (2011d) reported a detailed study of the behaviour of the flare-like events of IGR J17091−3624 during the first 180 d of the outburst. This study classified the different types of flares with the same scheme as used by Belloni et al. (2000) for GRS 1915+105.

In this paper, we report on the *Swift* and *INTEGRAL* data analysis of the new outburst of IGR J17091−3624 started at the end of 2011 January.

2 DATA REDUCTION AND ANALYSIS

The XRT ToO follow-up observations were performed, when possible, simultaneously to the *INTEGRAL* ones (Capitanio et al. 2011). *INTEGRAL* data were collected in the framework of the Galactic bulge observations[1] (public data) and the open time observation of the RX J1713.7−3946 field. Due to the long duration of the outburst, *Swift*/XRT data were also collected in the period in which the region around IGR J17091−3624 became unobservable by *INTEGRAL*. In this paper, we made use of the whole available data set of *INTEGRAL* and *Swift* observations performed from 2011 January 28 to 14 August.

The XRT observations were taken in window timing mode in order to avoid the pile-up effects. Each observation was composed of two or more segments. We reported only the analysis of the first segments of all XRT observations, since the other segments were always consistent with the first segments of each observation. For the XRT data analysis we followed standard procedures (Burrows et al. 2005) and the technique summarized in Bozzo et al. (2009). XRT light curves and the hardness–intensity diagrams (HIDs) were obtained from the XRT data extracting two different energy ranges, 0.3–4 and 4–10 keV.

For the *INTEGRAL* data analysis, we used the latest release of the standard Offline Scientific Analysis, OSA version 9.0, distributed by the *INTEGRAL* Science Data Centre (Courvoisier et al. 2003) and the latest response matrices available. In particular, the IBIS response matrices were produced using the closest available Crab observations to the 2011 outburst of IGR J17091−3624. Our *INTEGRAL* analysis was focused on ISGRI (Lebrun et al. 2003), the low-energy detector of the γ-ray telescope IBIS (Ubertini et al. 2003) and on the X-ray monitor JEM-X (Lund et al. 2003). Unfortunately, due to the *INTEGRAL* observing strategy combined to the small JEM-X field of view (FOV), IGR J17091−3624 was not in the JEM-X FOV in most of the observations. During the *INTEGRAL* observations, both JEM-X modules were switched on. However, for the data analysis we used the second module (JEM-X2) and checked the consistency with module 1. The ISGRI and JEM-X spectra were extracted in 20–200 and 3–20 keV, respectively. A systematic error of 2 per cent was taken into account for spectral analysis (see also Jourdain et al. 2008).

Details on all the *Swift* and *INTEGRAL* data analysed in this paper are given in Table 1 (columns 1–4). The spectral and timing analysis have been performed with the HEASOFT 6.9 package. In particular, the periods of the flare-like events were calculated with the FTOOL efsearch. The rms values were estimated from the source light curves by using an ad hoc developed tool and the IDL Astronomy User's Library procedures.[2] For the rms calculation, we divided the light curves, extracted in 1-s bins, into 140-s chunks. For each segment we computed the fractional rms after subtracting the expected white noise. We then estimated the fractional rms of the light curves and its uncertainty from the average and standard deviation of the single determinations. The effective frequency range over which the rms is integrated is therefore 0.007–0.5.

3 RESULTS

The 2011 outburst of IGR J17091−3624 can be divided into two main phases: during the first phase, the source underwent the typical sequence of events of a transient BH in outburst (described in Section 3.1); during the second phase, it exhibited 'heartbeat' variability previously observed only in GRS 1915+105 (Sections 3.2 and 3.3). Finally, a detailed study on the presence of a Compton reflection component and iron line upper limit is given in Section 3.4.

3.1 The initial phases of the outburst

The outburst of IGR J17091−3624 started on MJD ∼55598 (Fig. 1) and in about 12 d the X-ray flux of the source (2–10 keV) increased to about 70 per cent. During this starting phase, the *Swift* and *INTEGRAL* simultaneous data, when available, could be well fitted by an absorbed cut-off power-law model. The source showed a typical hard state spectrum and the photon index and high-energy cut-off remained consistent within the errors ($\Gamma \sim 1.5, E_{\rm c} \sim 100$ keV, see Table 1 for details). The equivalent hydrogen column density value

---

[1] http://integral.esac.esa.int/BULGE

[2] http://idlastro.gsfc.nasa.gov/

Table 1. Observations log and spectral parameters of the outburst evolution. Note that all the errors are at the 90 per cent confidence level. N is the label of each XRT observation associated with the points of Figs 5 and 11; ID is the XRT observation number; date is the date of the XRT observation; XRT EXP indicates the exposure time of the XRT observation. *INTEGRAL* REV indicates, when available, the revolution number of *INTEGRAL* simultaneous observations; rms is the value of the rms amplitude of each XRT observations averaged in an interval between 0.007 and 0.5 Hz. $T_{\rm in}$ is the inner temperature of the diskbb model in XSPEC; NORM diskbb is the normalization of the diskbb model proportional to the square of the inner disc radius; Γ is the power-law photon index; and $E_{\rm c}$ is the high-energy cut-off; $\mathrm{Flux}_{(2-10)\,\mathrm{keV}}$ is the unabsorbed flux between 2 and 10 keV.

N	ID	Date (MJD)	XRT EXP (s)	*INTEGRAL* REV	rms (count)	$T_{\rm in}$ (keV)	NORM diskbb	Γ	$E_{\rm c}$ (keV)	$\mathrm{Flux}_{(2-10)\,\mathrm{keV}}$ ($\times 10^{-10}$ erg cm^{-2} s^{-1})	$\chi^2_{\rm red}$(d.o.f.)
1	00031921002	55598.3	1940	1016	0.29 ± 0.08	–	–	$1.4^{+0.1}_{-0.1}$	109^{+28}_{-19}	6.1	1.0(139)
2	00031921003	55599.2	2170	1016	0.28 ± 0.03	–	–	$1.5^{+0.1}_{-0.1}$	120^{+30}_{-21}	6.5	1.0(193)
3	00031921004	55600.7	2175	1016	0.25 ± 0.07	–	–	$1.5^{+0.1}_{-0.1}$	104^{+19}_{-14}	6.8	1.0(164)
4	00031921005	55601.1	1454	–	0.25 ± 0.06	–	–	$1.5^{+0.1}_{-0.1}$	–	6.1	0.8/175)
5	00031921006	55602.1	2191	1017	0.21 ± 0.03	–	–	$1.6^{+0.1}_{-0.1}$	125^{+31}_{-21}	9.3	1.0(174)
6	00031921007	55603.2	2066	1017	0.24 ± 0.06	–	–	$1.5^{+0.1}_{-0.1}$	86^{+11}_{-9}	8.6	1.0(210)
7	00031921008	55604.2	2189	1017	0.27 ± 0.03	–	–	$1.5^{+0.1}_{-0.1}$	93^{+11}_{-9}	9.4	1.3(264)
8	00031921009	55605.2	2163	1018	0.24 ± 0.07	–	–	$1.5^{+0.1}_{-0.1}$	86^{+35}_{-21}	10.0	1.1(200)
9	00031921010	55606.2	1884	–	0.22 ± 0.03	–	–	$1.6^{+0.1}_{-0.1}$	–	8.6	1.1(139)
10	00031921011	55607.2	2108	–	0.24 ± 0.05	–	–	$1.6^{+0.1}_{-0.1}$	–	8.9	1.1(217)
11	00031921012	55608.3	2057	–	0.22 ± 0.02	–	–	$1.61^{+0.04}_{-0.04}$	–	9.1	1.1(249)
12	00031921013	55610.2	2010	–	0.21 ± 0.03	–	–	$1.6^{+0.1}_{-0.1}$	–	10.4	1.0(225)
13	00031921014	55612.3	2095	1020	0.15 ± 0.05	–	–	$1.69^{+0.04}_{-0.04}$	75^{+9}_{-7}	14.7	1.0(311)
14	00031921015	55614.2	2195	1020	0.08 ± 0.04	$0.3^{+0.1}_{-0.1}$	$<1 \times 10^5$	$2.0^{+0.1}_{-0.1}$	134^{+43}_{-29}	20.5	1.2(366)
15	00031921016	55616.3	1074	–	0.05 ± 0.02	$1.1^{+0.1}_{-0.1}$	53^{+38}_{-24}	$2.1^{+0.3}_{-0.5}$	–	20.6	1.1(322)
16	00031921017	55620.8	2568	–	0.06 ± 0.02	$1.0^{+0.1}_{-0.1}$	54^{+35}_{-25}	$2.1^{+0.2}_{-0.2}$	–	17.8	1.0(428)
17	00031921018	55622.5	2321	–	0.09 ± 0.03	$1.0^{+0.2}_{-0.1}$	46^{+63}_{-37}	$2.1^{+0.3}_{-0.4}$	–	19.5	1.2(268)
18	00031921019	55623.5	656	–	0.05 ± 0.02	$1.1^{+0.2}_{-0.1}$	54^{+41}_{-27}	$2.1^{+0.3}_{-0.4}$	–	18.2	1.1(316)
19	00031921020	55624.4	2463	–	0.05 ± 0.02	$1.1^{+0.1}_{-0.1}$	60^{+18}_{-18}	$1.7^{+0.3}_{-0.7}$	–	18.9	1.1(443)
20	00031921021	55627.6	2072	1025	0.04 ± 0.02	$1.3^{+0.1}_{-0.1}$	49^{+24}_{-14}	$2.4^{+0.1}_{-0.1}$	–	35.1	1.0(433)
21	00031921022	55628.1	1706	1025	0.05 ± 0.02	$1.29^{+0.04}_{-0.04}$	98^{+56}_{-30}	$2.4^{+0.2}_{-0.1}$	–	47.6	1.1(489)
22	00031921023	55630.5	1408	–	0.05 ± 0.02	$1.03^{+0.05}_{-0.04}$	90^{+13}_{-19}	$1.3^{+0.5}_{-0.1}$	–	17.1	1.2(401)
23	00031921024	55632.3	2189	1027	0.07 ± 0.02	$1.29^{+0.04}_{-0.04}$	71^{+33}_{-21}	$2.6^{+0.1}_{-0.1}$	–	40.3	1.0(411)
24	00031921025	55633.3	2016	–	0.08 ± 0.06	$1.31^{+0.02}_{-0.02}$	51^{+4}_{-4}	–	–	18.2	1.2(357)
25	00031921026	55635.6	1473	1028	0.07 ± 0.03	$1.2^{+0.1}_{-0.1}$	35^{+12}_{-8}	$2.1^{+0.1}_{-0.1}$	–	15.2	1.2(434)
26	00031921028	55639.8	2225	–	0.27 ± 0.02	$1.28^{+0.03}_{-0.03}$	63^{+20}_{-26}	–	–	20.7	1.0(274)
27	00031921029	55638.6	2155	–	0.10 ± 0.02	$1.29^{+0.02}_{-0.02}$	54^{+3}_{-3}	–	–	18.7	1.0(417)
28	00031921030	55640.5	2348	–	0.28 ± 0.02	$1.29^{+0.02}_{-0.02}$	57^{+3}_{-3}	–	–	19.2	1.3(442)
29	00031921031	55642.1	2137	1030	0.26 ± 0.01	$1.32^{+0.03}_{-0.03}$	47^{+4}_{-4}	–	–	25.6	1.0(308)
30	00031921033	55643.4	630	1030	0.11 ± 0.06	$1.2^{+0.1}_{-0.1}$	64^{+138}_{-31}	$2.1^{+0.3}_{-0.2}$	–	23.6	1.1(314)
31	00031921034	55646.9	2166	–	0.12 ± 0.02	$1.29^{+0.02}_{-0.02}$	45^{+3}_{-3}	–	–	15.0	1.2(382)
32	00031921036	55650.2	326	–	0.192 ± 0.003	$1.28^{+0.04}_{-0.04}$	51^{+6}_{-6}	–	–	16.9	0.9(196)
33	00031921037	55651.5	2067	1033	0.22 ± 0.02	$1.2^{+0.1}_{-0.1}$	55^{+91}_{-25}	$2.1^{+0.2}_{-0.3}$	–	17.4	1.0(288)
34	00031921038	55654.7	1173	1034	0.31 ± 0.01	$1.27^{+0.04}_{-0.10}$	74^{+163}_{-41}	$2.4^{+0.2}_{-0.3}$	–	29.6	1.2(424)
35	00031921039	55655.7	1022	–	0.31 ± 0.02	$1.31^{+0.02}_{-0.02}$	52^{+4}_{-4}	–	–	18.8	1.1(397)
36	00031921040	55657.5	2111	1035	0.31 ± 0.01	$1.22^{+0.09}_{-0.10}$	57^{+140}_{-30}	$2.6^{+0.4}_{-0.4}$	–	23.4	0.8(216)
37	00031921041	55661.9	974	–	0.32 ± 0.02	$1.31^{+0.02}_{-0.02}$	45^{+3}_{-3}	–	–	16.6	1.1(382)
38	00031921042	55667.3	1069	–	0.34 ± 0.04	$1.29^{+0.02}_{-0.02}$	48^{+3}_{-3}	–	–	16.7	1.2(387)
39	00031921043	55679.8	896	–	0.33 ± 0.02	$1.29^{+0.02}_{-0.02}$	48^{+4}_{-3}	–	–	16.1	1.2(359)
40	00031921044	55681.2	1035	–	0.26 ± 0.04	$1.29^{+0.02}_{-0.02}$	44^{+3}_{-3}	–	–	15.0	1.1(375)
41	00031921045	55683.7	1509	–	0.15 ± 0.03	$1.25^{+0.02}_{-0.02}$	52^{+3}_{-3}	–	–	15.1	1.2(397)
42	00031921046	55685.3	1246	–	0.05 ± 0.01	$1.26^{+0.03}_{-0.03}$	49^{+5}_{-5}	–	–	13.2	1.1(231)
43	00031921049	55691.6	2092	–	0.08 ± 0.06	$1.1^{+0.2}_{-0.1}$	37^{+31}_{-16}	2^{+1}_{-2}	–	10.9	0.9(198)
44	00031921050	55693.1	2318	–	0.08 ± 0.04	$1.0^{+0.1}_{-0.1}$	62^{+9}_{-15}	1^{+1}_{-2}	–	9.7	1.0(311)
45	00031921051	55695.0	1139	–	0.08 ± 0.03	$1.2^{+0.2}_{-0.2}$	15^{+19}_{-9}	$2.4^{+0.3}_{-0.3}$	–	9.1	1.0(303)
46	00031921052	55697.8	1160	–	0.07 ± 0.04	$1.1^{+0.2}_{-0.1}$	26^{+23}_{-12}	$2.4^{+0.3}_{-0.4}$	–	8.7	1.2(298)
47	00031921053	55701.8	1188	–	0.10 ± 0.02	$1.1^{+0.2}_{-0.1}$	20^{+19}_{-10}	$2.4^{+0.3}_{-0.4}$	–	8.6	1.1(300)

Table 1 – *continued*

N	ID	Date (MJD)	XRT EXP (s)	*INTEGRAL* REV	rms (count)	$T_{\rm in}$ (keV)	NORM diskbb	Γ	$E_{\rm c}$ (keV)	$\mathrm{Flux}_{(2-10)\,\mathrm{keV}}$ ($\times 10^{-10}$ erg cm^{-2} s^{-1})	$\chi^2_{\rm red}$(d.o.f.)
48	00031921054	55703.7	2291	–	0.08 ± 0.02	$1.0^{+0.2}_{-0.1}$	30^{+23}_{-19}	–	–	9.6	1.0(299)
49	00031921055	55705.6	2374	–	0.15 ± 0.03	$1.23^{+0.02}_{-0.02}$	49^{+4}_{-3}	–	–	13.6	1.1(375)
50	00031921056	55707.4	1789	–	0.26 ± 0.02	$1.24^{+0.02}_{-0.02}$	50^{+3}_{-3}	–	–	14.4	1.1(386)
51	00035096002	55715.7	894	–	0.18 ± 0.04	$1.27^{+0.02}_{-0.02}$	47^{+4}_{-4}	–	–	14.7	1.3(345)
52	00035096003	55717.7	1006	–	0.12 ± 0.02	$1.20^{+0.02}_{-0.02}$	46^{+4}_{-3}	–	–	11.3	1.3(334)
53	00035096004	55719.5	907	–	0.13 ± 0.05	$1.23^{+0.02}_{-0.02}$	45^{+4}_{-3}	–	–	12.3	1.1(323)
54	00035096005	55721.3	1070	–	0.17 ± 0.02	$1.24^{+0.02}_{-0.02}$	49^{+4}_{-37}	–	–	13.9	1.1(369)
55	00035096009	55725.6	1151	–	0.06 ± 0.03	$1.20^{+0.02}_{-0.02}$	46^{+4}_{-3}	–	–	9.0	1.3(334)
56	00035096010	55729.4	1006	–	0.07 ± 0.04	$1.3^{+0.3}_{-0.3}$	8^{+13}_{-3}	$2.5^{+0.9}_{-0.4}$	–	7.8	1.0(247)
57	00035096012	55731.0	437	–	0.07 ± 0.05	$1.09^{+0.04}_{-0.02}$	18^{+42}_{-12}	2^{+1}_{-1}	–	8.1	0.8(132)
58	00035096014	55733.2	928	–	0.11 ± 0.05	$1.0^{+0.1}_{-0.1}$	43^{+26}_{-19}	2^{+1}_{-5}	–	7.8	1.0(238)
59	00035096015	55735.3	1102	–	0.10 ± 0.03	$1.1^{+0.1}_{-0.1}$	49^{+30}_{-13}	3^{+1}_{-1}	–	12.5	1.1(283)
60	00035096016	55737.5	140	–	0.16 ± 0.04	$1.2^{+0.1}_{-0.1}$	51^{+19}_{-14}	–	–	11.8	1.0(46)
61	00035096017	55739.4	992	–	0.32 ± 0.05	$1.2^{+0.03}_{-0.03}$	33^{+4}_{-3}	–	–	8.1	0.9(224)
62	00035096018	55741.6	1123	–	0.39 ± 0.03	$1.47^{+0.03}_{-0.03}$	25^{+2}_{-2}	–	–	15.2	1.3(375)
63	00035096019	55744.0	984	–	0.37 ± 0.02	$1.58^{+0.04}_{-0.04}$	19^{+2}_{-2}	–	–	17.2	1.1(350)
64	00035096020	55759.3	850	–	0.36 ± 0.05	$1.67^{+0.06}_{-0.05}$	18^{+2}_{-2}	–	–	19.6	1.1(210)
65	00035096021	55761.5	727	–	0.42 ± 0.03	$1.50^{+0.04}_{-0.03}$	24^{+2}_{-2}	–	–	16.1	1.2(311)
66	00035096022	55765.3	956	–	0.41 ± 0.04	$1.35^{+0.03}_{-0.03}$	36^{+3}_{-3}	–	–	15.0	1.0(363)
67	00035096023	55767.3	940	–	0.38 ± 0.04	$1.32^{+0.02}_{-0.02}$	37^{+3}_{-3}	–	–	14.0	1.1(346)
68	00035096027	55775.3	863	–	0.39 ± 0.03	$1.34^{+0.03}_{-0.02}$	38^{+3}_{-3}	–	–	15.3	1.1(342)
69	00035096028	55777.9	354	–	0.22 ± 0.01	$1.27^{+0.04}_{-0.04}$	47^{+7}_{-6}	–	–	14.9	1.2(165)
70	00035096029	55779.4	511	–	0.23 ± 0.06	$1.24^{+0.04}_{-0.03}$	50^{+6}_{-5}	–	–	14.3	1.0(237)
71	00035096030	55783.8	547	–	0.34 ± 0.03	$1.30^{+0.04}_{-0.04}$	82^{+11}_{-10}	–	–	29.0	1.1(198)
–	–	55785.0	–	1078	–	$1.3^{+0.1}_{-0.1}$	58^{+32}_{-20}	$2.3^{+0.2}_{-0.2}$	–	24.7	1.1(26)
72	00035096032	55787.7	974	–	0.37 ± 0.04	$1.28^{+0.02}_{-0.02}$	58^{+5}_{-5}	–	–	19.2	1.1(352)

was consistent with the one reported by Krimm & Kennea (2011), $N_{\rm H} = (1.1 \pm 0.3) \times 10^{22}$ cm^{-2}.

Fig. 2 shows the combined XRT–ISGRI unfolded LHS spectrum along with the residuals expressed in terms of sigmas (MJD 55603.2, observation no. 6 in Table 1).

On MJD ~55610.2, the source displayed evidence for the beginning of a spectral transition to the softer state. The flux continued to increase more rapidly: ~100 per cent from observation 12 until observation 15 (about 6 d). But, this time, a significant softening of the hard X-ray spectrum (see e.g. the bottom panel of Fig. 1) was observed, together with a drop in the hard X-ray flux.

During the transition, the spectra became steeper and in about 2 d the fit required a multicolour disc blackbody component (MDBB, modelled with diskbb in XSPEC; Mitsuda et al. 1984). Fig. 3 shows two spectra extracted at the intermediate hardness values (hardness ratio, HR, ~0.2, observations 13 and 14). An acceptable fit to these spectra could be obtained by using an absorbed cut-off power-law model). Adding the MDBB component, the F-test probability of a chance improvement is 7 and 0.4 per cent for observations 13 and 14, respectively. Thus, it is reasonable to add an MDBB component only to the second spectrum.

The obtained spectral parameters of the spectrum 14 are compatible with the intermediate spectral states of a BHC (see e.g. Fender, Belloni & Gallo 2004; Remillard & McClintock 2006, and references therein). During the transition from the hard to the soft state, the inner temperature of the MDBB component ($kT_{\rm in}$) increased from 0.3 (observation 14) to ~1 keV (observations 15 and 16), while its normalization decreased significantly.[3]

At the end of the transition to the soft state (observation 16), the disc temperature reached a value of about 1 keV, while the power-law photon index reached ~2.1, with no cut-off detectable up to about 200 keV (see Table 1 for details). The fractional rms amplitude of the X-ray emission from IGR J17091−3624 as measured by XRT data decreased from previous values (25–30 per cent) up to about 4–5 per cent (see Fig. 5). Thus, as also reported by Del Santo et al. (2011), the source is probably in the HSS. In the following 65 d (until observation 42), the spectral characteristics of the source showed no significant variability. Fig. 4 shows the unfolded spectrum of IGR J17091−3624 after the transition (observation 33). The fit to these data was obtained with an absorbed MDBB plus a simple power-law component. No Compton reflection from the disc surface and no iron line models were required by the data even though these components are usually expected to be very strong in the canonical soft state of BH binaries (Gierlinsky et al. 1999).

On MJD 55655.8 (observation 34) a short flare, reaching a peak flux of 3×10^{-9} erg cm^{-2} s^{-1} (2–10 keV), was detected. No

---

[3] In the MDBB model (Mitsuda et al. 1984), the square root of the normalization constant is proportional to the apparent inner radius of the truncated disc. However, when the high-energy behaviour of the spectrum is modelled with a power-law component, the evolution of the disc internal radius can be significantly underestimated (see e.g. Done, Gierlinski & Kubota 2007, pages 28 and 29).

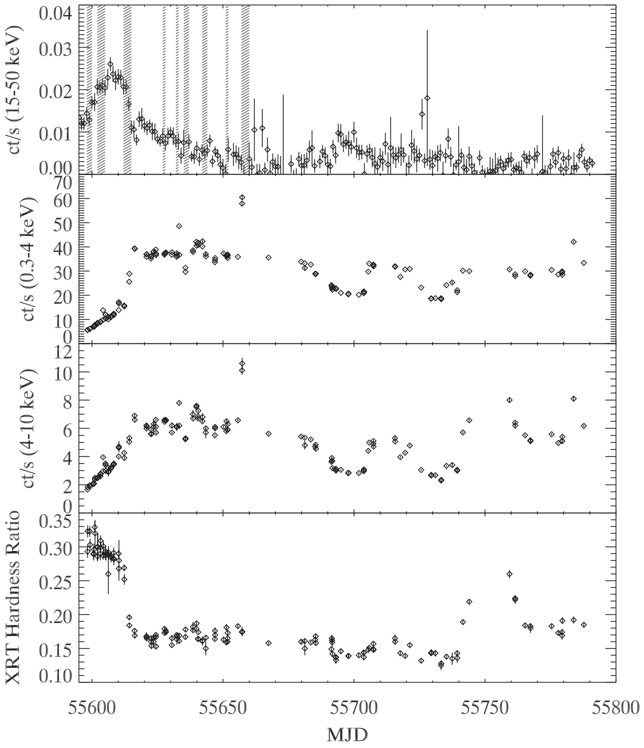

Figure 1. Top panel: *Swift*/BAT (15–50 keV) count rate (bin time = 1 d). The shadowed parts represent the *INTEGRAL* observation periods. Second panel: XRT (0.3–4 keV) count rate (bin time = 4000 s). Third panel: XRT (4–10 keV) count rate (bin time = 4000 s). Bottom panel: XRT hardness ratio (defined as the ratio between the 4–10 keV and the 0.3–4 keV count rates).

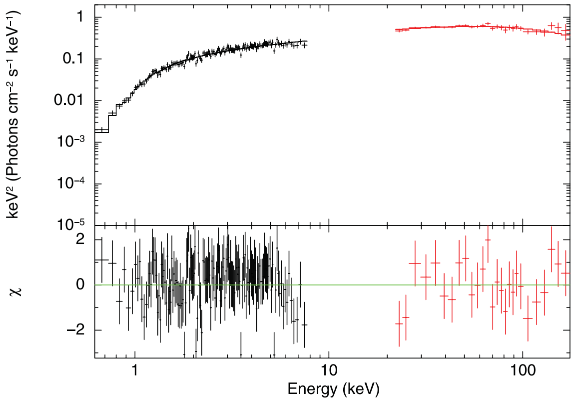

Figure 2. *Swift*/XRT and *INTEGRAL*/IBIS joint unfolded spectrum at the beginning of the outburst. The source presents a typical LHS spectrum (observation 3 in Table 1).

significant changes in the spectral properties of the source were detected during this event.

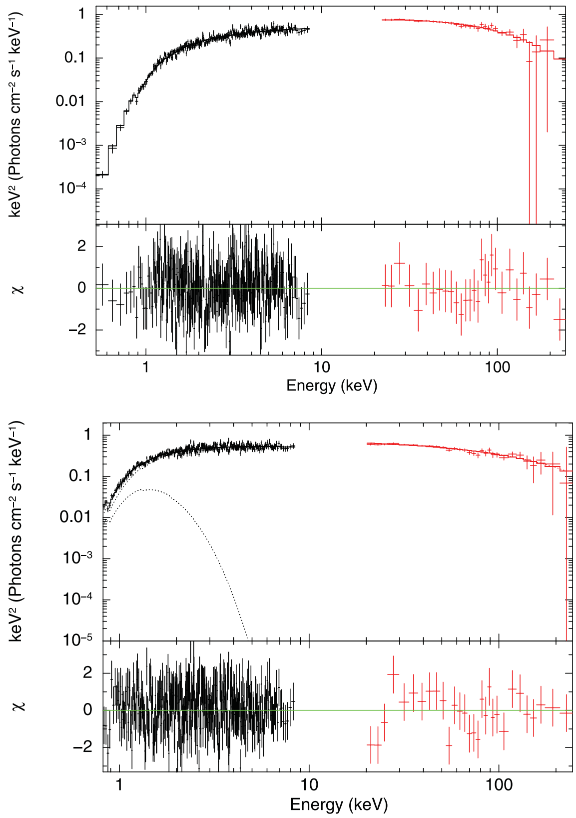

Figure 3. Two *Swift*/XRT and *INTEGRAL*/IBIS joint intermediate spectra during the transition from the LHS to the HSS. The two spectra have been collected from data separated by 2 d. Top spectrum: observation 13 in Table 1. Bottom spectrum: observation 14 in Table 1.

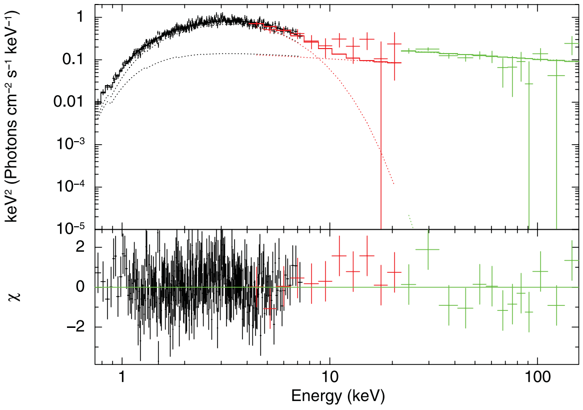

Figure 4. *Swift*/XRT *INTEGRAL*/JEM-X2 and *INTEGRAL*/IBIS unfolded spectra of the IGR J17091−3624 soft state (see Section 4). The fit is an absorbed MDBB plus a power law. No reflection component is needed in the fit (the spectral parameter values are reported in Table 1, observation 33).

3.2 The appearance of the 'heartbeat'

Fig. 5 shows the fractional rms amplitude as a function of the HR.[4] As mentioned above, during the transition from the hard to the soft state, the fractional rms and the HR decreased as expected by a typical transient BH entering the HSS (Fender et al. 2004).

However, from observation 26 the fractional rms amplitude moved away from the expected values and started to increase and decrease rapidly with a chaotic behaviour (see e.g. Fig. 5). The rapid increases correspond to the observations in which the quasi-periodic flare-like events are detected in the light curves (the 'heartbeat' in

---

[4] We defined as the HR the ratio of the counts in the 4–10 keV energy band to the counts in the 0.3–4 keV energy band in each XRT observation.

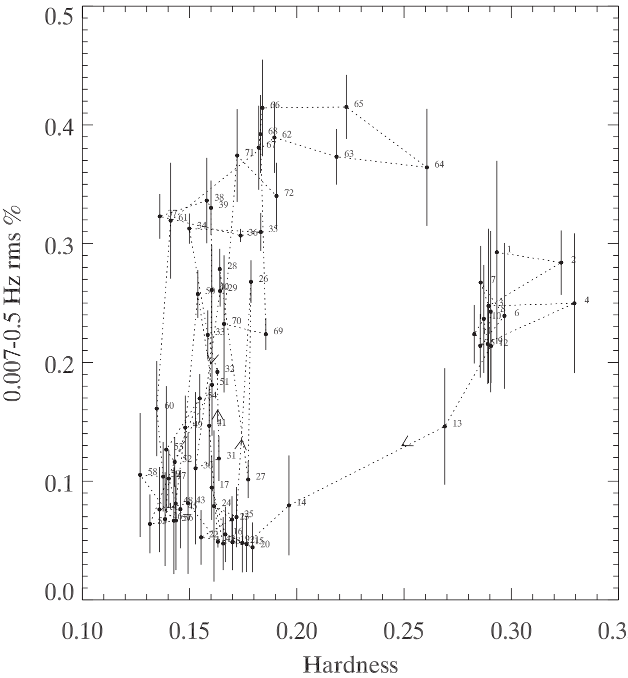

Figure 5. Hardness–rms diagram of each XRT pointing of the IGR J17091−3624 outburst. For the observations with more than one segment, only the first one has been considered. For the usage of rms as a tracer of the different accretion regimes see e.g. Munoz-Darias, Motta & Belloni (2011) and Capitanio et al. (2009b). In order to get a more readable figure, we did not show the hardness error bars that are, instead, reported in Fig. 11.

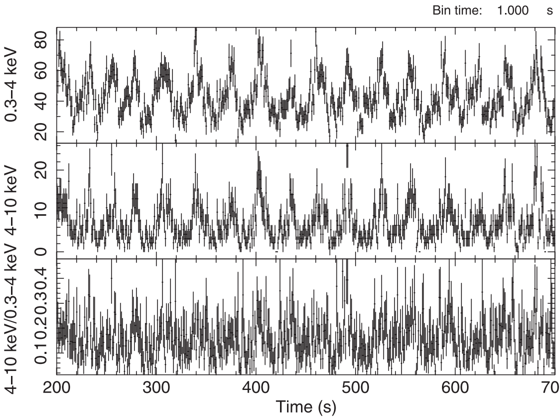

Figure 6. Zoom of the XRT count rate of observation 28 in Table 1. The time bin is 1 s and the start time is MJD 55640.5.

analogy with GRS 1915+105, see also Section 1). As an example, Fig. 6 shows a zoom of the light curve of one of the XRT observations in which the ‘heartbeat’ is detected. The ‘heartbeat’ oscillations vary in intensity and hardness; in some observations, they are not detected at all (in these cases lower values of the fractional rms amplitude are measured). No significative variations can be observed in the spectra of each XRT observation with or without the presence of the ‘heartbeat’. We also observed that the flare-like events lose coherence and change their period with time. Fig. 7 shows the evolution of the ‘heartbeat’ period as a function of time. This behaviour is consistent with that observed with *RXTE* (Altamirano et al. 2011c,d). The two panels of Fig. 8 show the ‘heartbeat’ period as a function of hardness and XRT count rate, respectively.

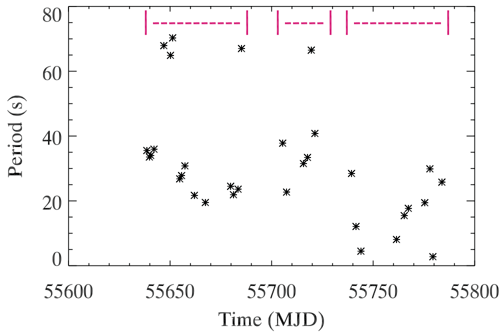

Figure 7. ‘Heartbeat’ period versus time. The dashed segments represent the three different groups of observations discussed in the text.

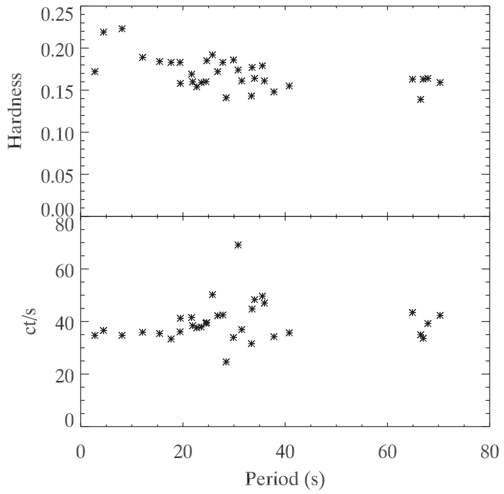

Figure 8. Top panel: hardness versus ‘heartbeat’ period. Bottom panel: XRT count rate versus ‘heartbeat’ period.

No evident correlation between the periods of the flare-like events with the count rate or the HR has been found. The only peculiarity is the presence of a sort of ‘forbidden zone’ in the possible period values (from ∼40 to ∼65 s, Figs 7 and 8). For a detailed discussion of the different ‘heartbeat’ states of IGR J17091−3624, see Altamirano et al. (2011d).

No significant detection of the ‘heartbeat’ was found in the IBIS light curve because of the faintness of the source in the hard X-ray domain (20–200 keV) and the relatively poor statistics.

After MJD ∼55690 (observations 43 and 44), the ‘heartbeat’ was no longer detected and at the same time the flux in the 15–50 keV energy band started to increase again (see the BAT light curve in Fig. 1). The spectral analysis of the observations performed during this period showed that the inner temperature of the MDBB component decreased down to ∼1 keV and a power-law component was also required in order to have an acceptable fit of the XRT spectra. In the previous observations, a power-law component additional to MDBB was required only when XRT and IBIS data were fitted simultaneously. Between observations 37 and 41 the *INTEGRAL* data were unavailable, and thus we could not constrain the properties of the source emission in the hard X-ray domain.

On MJD 55705.6 (observation 49), the 15–50 keV light curve started to decrease again. Correspondingly, the soft XRT light curve increases significantly (see Fig. 1) and the XRT spectra reached again approximately the same shape as observed during the

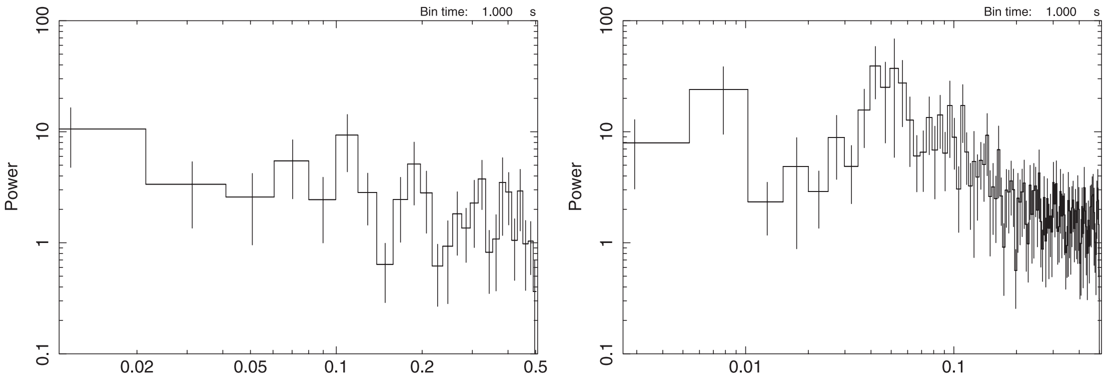

(a) id: 00035096016 (b) id: 00035096017

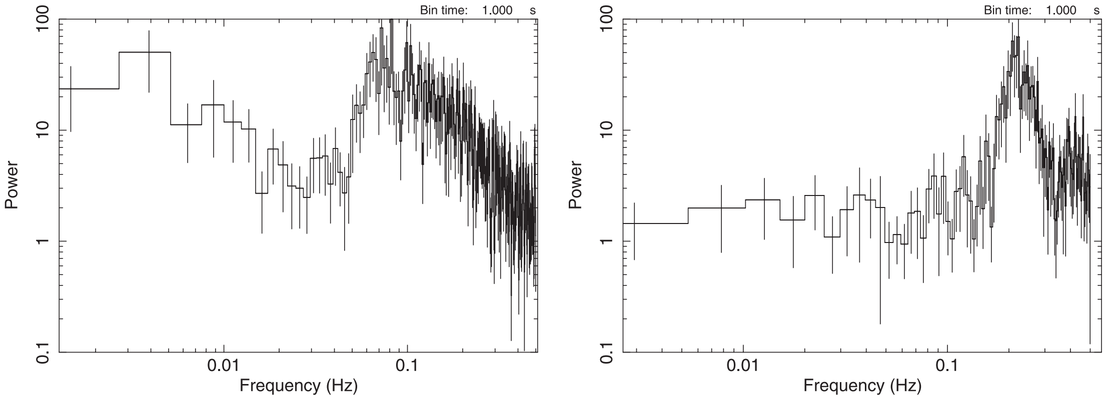

(c) id: 00035096018 (d) id: 00035096019

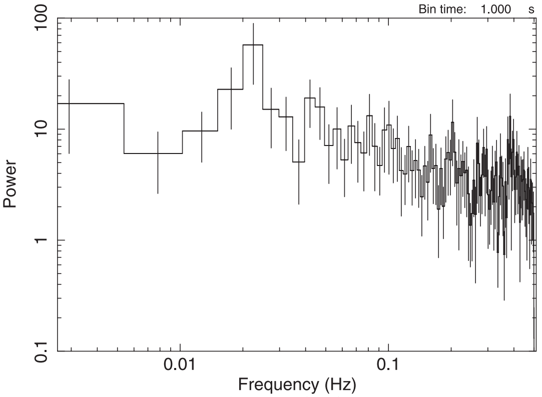

(e) id: 00035096020

Figure 9. XRT power spectra evolution of five observations (binned at 1s), from MJD 55737.5 to 55759.3 (observations 60–64), that correspond to the reappearance of the flare-like events of the last part of the XRT campaign of IGR J17091−3624.

previously detected soft state. On the same date, MJD 55705.6, a second group of recurrent flare-like events appeared again in the light curves. At this time, the flux variation of the flare events was less pronounced and less coherent, while the periods scanned approximately the same range as in the previous group of events (see Fig. 7).

As Fig. 1 shows, from MJD∼55730 until 55770 there was an increase in the XRT flux together with a sharp hardening. The consequence of the hardening in the XRT spectra is an increase of the inner disc temperature and a decrease of the normalization constant of the MDBB model, NORM, that reached values of about ∼18 (see Table 1). In particular, NORM is proportional to the square of the apparent inner disc radius and to cos$i$, where i is the angle between the disc and the observer (Mitsuda et al. 1984).[5] Thus, in order to obtain an inner radius with a plausible length, cos$i$ should be very small. Simultaneously to the spectral hardening, the XRT light curves and the corresponding power spectra clearly showed that a third group of recurrent flare-like events started with a remarkably decreased period (see Fig. 7).

As an example, the five panels of Fig. 9 show the XRT power spectra evolution, from MJD 55737.5 to 55759.3 (observations 60–64). This time interval corresponds to the reappearance of the

---

[5] The connection between the apparent inner disc radius and the inner radius itself is reported by Kubota et al. (1998).

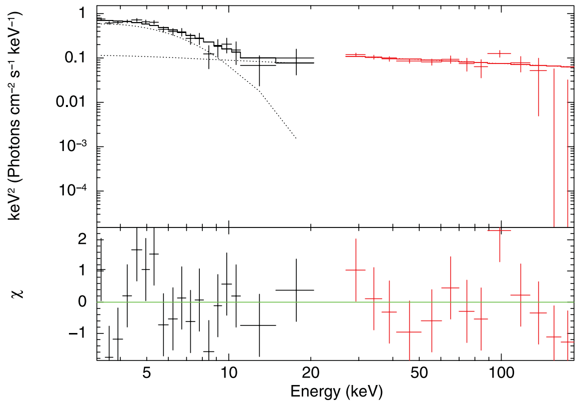

Figure 10. *INTEGRAL*/JEM-X2 and *INTEGRAL*/IBIS-averaged spectrum of IGR J17091−3624 in the soft state during revolution 1078 (MJD 55785.0). The fit is an absorbed MDBB plus a power law. The spectral parameters are reported in Table 1.

flare-like events: at MJD 55737.3 (observation 60), there were no flare-like events and the power spectrum presented a power-law-like behaviour (Fig. 9a). On MJD 55741.6, the flare-like events started again and a prominent and broad feature appeared in the power spectrum shape (Figs 9b and c). The frequency of this feature changed with time from ~0.72 to ~0.22 Hz (Figs 9d and e).

The 'heartbeat' is always detected during the final part of the *Swift* campaign with periods spanning from about 3 until 30 s. The energy spectra of each single XRT observation were fitted with the same model as before (absorbed multicolour disc blackbody plus a power-law component). However, after observation 65, the inner temperature of the MDBB component decreased from ~1.5 to ~1.3 keV (see Table 1 for details). The *INTEGRAL* observations, performed during revolution 1078 (MJD 55785.0), showed that the fit of the hard part of the spectrum is consistent with a simple power-law component with a photon index of $\Gamma = 2.3 \pm 0.2$ (see Fig. 10).

We also note that during the periods in which IGR J17091−3624 displayed evidence for the 'heartbeat' phenomena, its spectral evolution remained trapped in the top left corner of the HID (see Fig. 11) and no longer outlined the canonical path through the different spectral states expected from a BHC in outburst (the so-called *q*-track).

3.3 Spectra from the 'heartbeat'

In order to investigate the origin of the changes in the hardness ratio during the 'heartbeat', we extracted XRT spectra in the time intervals corresponding to the highest (>60 count s^{-1}) and lowest (<30 count s^{-1}) count rates of the source spectra during the flaring activity. For these data, we performed a rate-resolved analysis adding up time intervals corresponding to the peaks and to the minima of the flare in each observation (note, however, that the hardening of the different peaks was not constant; see for example the HR behaviour in Fig. 6). Because of the periodicity of the light curve, the rate-resolved analysis overlaps with the phase-resolved analysis.

A fit to the spectra was obtained by using an absorbed MDBB component. The spectral parameters at highest count rates indicated

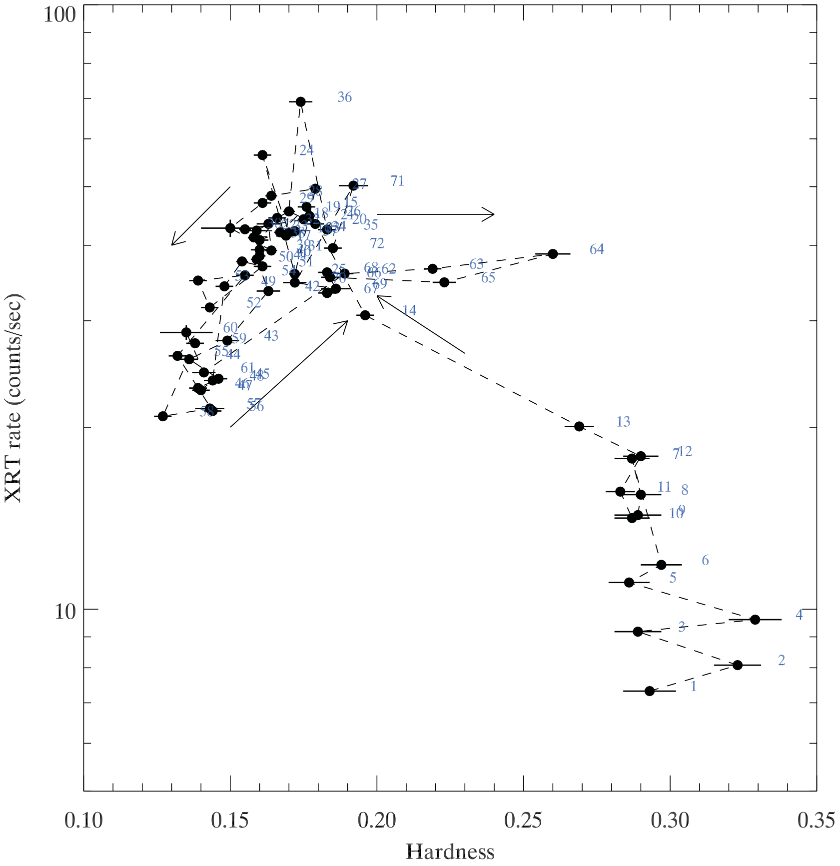

Figure 11. HID of all the XRT 2011 outburst observations of IGR J17091−3624. For the observations with more than one segment, only the first one has been considered.

Table 2. Spectral parameters of the different phases of three XRT observations: N is the number of the XRT observation as in Table 1; H: maxima count rate intervals (>60 count s^{-1}); L: minima count rate intervals (<30 count s^{-1}).

N	ID	Phase	T_{in} (keV)	NORM diskbb	$F_{(0.1-10\,\mathrm{keV})}$ ($\times 10^{-9}$ erg cm^{-2} s^{-1})	$\chi^2_{\mathrm{red.}}$	d.o.f.
26	00031921028	H	$1.4^{+0.1}_{-0.1}$	69^{+12}_{-10}	6	1.04	67
26	00031921028	L	$1.1^{+0.1}_{-0.1}$	81^{+27}_{-21}	2	1.17	24
28	00031921030	H	$1.49^{+0.03}_{-0.03}$	52^{+4}_{-4}	6	0.99	212
28	00031921030	L	$1.10^{+0.03}_{-0.03}$	63^{+8}_{-7}	2	1.02	83
38	00031921042	H	$1.6^{+0.1}_{-0.1}$	37^{+5}_{-4}	5	0.88	112
38	00031921042	L	$1.00^{+0.02}_{-0.02}$	83^{+8}_{-7}	2	0.98	128
51	00035096002	H	$1.4^{+0.1}_{-0.1}$	52^{+12}_{-10}	4	0.85	42
51	00035096002	L	$1.18^{+0.03}_{-0.03}$	46^{+5}_{-4}	2	1.00	126
54	00035096005	H	$1.5^{+0.1}_{-0.1}$	38^{+8}_{-7}	4	1.3	64
54	00035096005	L	$1.23^{+0.03}_{-0.03}$	40^{+3}_{-3}	2	1.10	185

a higher inner disc temperature and a hint for a smaller inner disc radius (see Table 2 for details) than what measured at lower count rates. This behaviour is more evident in some observations of the first group of data showing recurrent flare-like events (between MJD ∼55630 and ∼55690), where the flux variation during the flares was more pronounced. In fact, unfortunately, due to the low data statistics, only in a few observations was it possible to constrain the MDBB normalization constant with enough confidence.

In the second group (from MJD ∼55700 to ∼55730) the changes in the HR with the source count rates and the coherence of the 'heartbeat' oscillation are less evident. We report in Table 2 the spectral parameters of three representative XRT observations selected at different time periods. The N_{H} is fixed to be the same for the different phases of the same observations.

The unfolded phase-resolved spectra obtained for the XRT observation 30 (MJD 55640.5) are shown in Fig. 12. We found evidence that the flares are due to an oscillation of the inner disc boundary (Table 2): at the peak of the flare, the MDBB temperature (radius) is higher (smaller) with the disc approaching the BH event horizon. The opposite behaviour is observed during the minima of the flare. This is similar to what has been observed in the case of GRS 1915+105 (Neilsen, Remillard & Lee 2011). The lower X-ray flux of IGR J17091−3624 with respect to GRS 1915+105, however, does not allow us to study the 'heartbeat' in the same details. Theoretical studies suggest that this phenomenon is due to the Lightman–Eardley instability, a limit cycle in the inner accretion disc-dominated by the radiation pressure (Lightman & Eardley 1974; Szuszkiewicz & Miller 1998; Nayakshin & Rappaport 2000). According to this interpretation, the inner part of the disc empties and refills with a time-scale of seconds (Belloni et al. 1997).

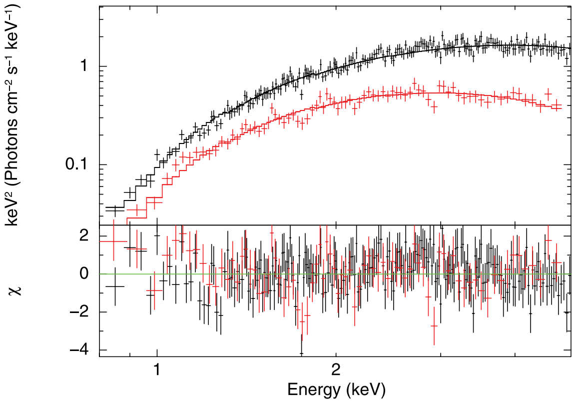

Figure 12. Count rate resolved spectra of observation 00031921030. The upper spectrum was extracted during time intervals corresponding to the peaks of the flare-like events observed in this observation. The lower spectrum corresponds to the time intervals of the flares where the source count rate was a minimum. The two spectra were fitted together with an unabsorbed MDBB model (we constrained N_{H} to be the same for the two spectra and we let the other parameters to vary independently).

3.4 Reflection component

In order to investigate the presence of a Compton reflection component and the iron line in the spectra of IGR J17091−3624, we used the XRT, JEM-X and IBIS joint spectra shown in Fig. 10. In this case the spectral parameters revealed that IGR J17091−3624 is in the soft state (observation 33) when the highest contribution from the reflection component is expected (see e.g. Ross & Fabian 2007, and reference therein). The model used to fit the data is an absorbed MDBB plus an exponentially cut-off power-law spectrum reflected by neutral material (pexrav in XSPEC; Magdziarz & Zdziarski 1995).

Considering the distance of the source estimated by Pahari et al. (2011b) and Rodriguez et al. (2011b), we also took into account the hypothesis that the source could belong to the Galactic halo and thus have a different metallicity with respect to the sources in the Galactic bulge, where normally LMXBs are concentrated (Grimm, Gilfanov & Suyaev 2002). No significant changes in the spectral fits were observed by leaving the metallicity of the reflecting medium free to vary. We thus assumed two different values of the metallicity, i.e. the solar one (the source belongs to Galactic bulge, $Z/Z_{\odot} = 1$) and $Z/Z_{\odot} = 0.13$ as reported by Frontera et al. (2001) for XTE J1118+480 which is a BH binary that lies at very high Galactic latitudes. In both cases, the estimated upper limit on the reflection component was of $R = 0.1$, and the F-test probability indicated that there is not a clear evidence of a significant improvement in χ^2 by adding this component (the F-test probability in the two cases was of 7 and 2 per cent, corresponding to a detection significance of $<2.0\sigma$ and $<2.5\sigma$, respectively).

We also estimated an upper limit on the normalization of the iron line fixing the centroid of the line at 6.7 keV. We assumed a broad line with $\sigma = 0.7$ keV as in the case of GRS 1915+105 (see e.g. Martocchia et al. 2002 and references therein). The obtained upper limit on the equivalent width is EQ < 0.9 keV.

4 DISCUSSION

All the outbursts of IGR J17091−3624 observed before 2011 were fainter and poorly observed compared to the last one. However, the source, in the limit of the instruments capability, displayed the typical spectral and temporal evolution (Capitanio et al. 2005, 2009a) expected from a canonical BHC (for details on the transient BHC outburst evolution, see e.g. Fender et al. 2004). The 'heartbeat' phenomenon appeared only during the last 2011 outburst. Indeed, using all the available archival XRT observations in the direction of IGR J17091−3624, we verified that no 'heartbeat' was visible during the previous outbursts of the source.

We summarize here the initial evolution phases of the outburst occurred on 2011. The source underwent to a transition from the LHS to the HSS moving from the bottom right corner of the HID to the top left corner (Fig. 11, observations 1–15):

(i) during this transition, the source reached the intermediate states and the radio flare reported by Rodriguez et al. (2011b) should be the signature of the transition from the HIMS to the SIMS (Fender et al. 2004);

(ii) the rms amplitude starting from values of about ∼30 per cent in the LHS decreased significantly, reaching values that span from 6 to 2 per cent (see Fig. 5 and column 6 in Table 1);

(iii) the spectrum became softer with the presence of a prominent disc blackbody component (starting from observation 15) with the high-energy cut-off no longer detectable up to 200 keV.

The source remained in the HSS for about 10 d (from MJD 55623.5 until 55633.3). Starting from MJD 55635, the source no more followed the standard evolution of a transient BHC in outburst: the properties of the X-ray spectra in each observation showed no significant variability, while the source displayed a sudden atypical timing variability in the form of flare-like events occurring at a 33-s period ('heartbeat'). The X-ray emission at the peak of these flares is typically harder than the average source emission (see the third panel of Fig. 6).

Starting from MJD 55692, we measured a progressive decrease of the MDBB inner temperature with a corresponding hardening of the source emission. At this time, the flare-like events were no longer visible in the light curve. The hardening continued uninterrupted for about two days, then the inner temperature of the disc started to increase again, leading to a clear increase in the soft X-ray flux and a decrease of the hard X-ray emission. At this epoch, the 'heartbeat' again became visible.

The last part of the data analysed presented a short-period oscillation (between 3 and 30 s) and also a particularly hot inner disc temperature with a very small MDBB normalization constant that corresponds to a small apparent inner radius. Between MJD 55740 and 55760, the 4–10 keV XRT flux increased significantly (a factor of 60 per cent). The peak in the 4–10 keV flux (see Fig. 1) corresponds to a peak in the inner disc temperature ($T_{\rm in} \sim 1.7$ keV on MJD 55759.3).

The period of the 'heartbeat' changed with time (Fig. 7) and it seems to have a decreasing trend.

4.1 Comparison with the BH binary GRS 1915+105

As reported by Altamirano et al. (2011d) and Pahari et al. (2011b), the behaviour of the source resembles what observed from GRS 1915+105 in the various flaring states. Thus, the principal common characteristic between these two sources is just the presence of pseudo-periodic flare-like events in the light curve, i.e. the so-called 'heartbeat'. The HR (bottom panel of Fig. 6) of IGR J17091−3624 is similar to the GRS 1915+105 one, in the sense that in both sources the modulation of the light curve is also projected in the HR (Neilsen et al. 2011). However, in the GRS 1915+105 case, the hardness variation seems more pronounced (see for example Naik et al. 2002). Our phase-resolved energy spectra of the XRT data revealed that the hardening of the source X-ray emission at the peak and at the lower part of each flare is similar to that measured in the case of GRS 1915+105 (see e.g. Belloni et al. 1997; Mineo, Massaro & Cusumano 2010) and thus it is probably due to the same physical phenomenon (Lightman & Eardley 1974).

The period of the 'heartbeat' also seems to vary with time in the same range of values as for the two sources, even though in GRS 1915+105 the period amplitude gets larger for long timescales. This does not seem to be the case for IGR J17091−3624. Indeed, as shown in Fig. 7, the period variation with time seems to decrease and, moreover, in the third group of observations (from MJD 55750 until the end), it reaches values of the order of a few seconds (∼3–5 s). These values were not observed in GRS 1915+105 (Neilsen et al. 2011).

Similar to GRS 1915+105, we also measured for IGR J17091−3624 particularly hot inner disc temperatures (in the case of GRS 1915+105, the temperature can reach even higher values; see e.g. Belloni et al. 1997; Muno, Morgan & Remillard 1999; Fender & Belloni 2004).[6] This property, together with a small inner radius of the disc blackbody spectrum in X-ray binaries, has been directly associated with high values of the BH spin (Zhang, Cui & Chen 1997; Devis, Done & Blaes 2006).

Besides all these similarities between GRS 1915+105 and IGR J17091−3624, a particularly striking difference is the X-ray flux intensity during the outbursts. This fact cannot be easily explained because, unlike GRS 1915+105, for IGR J17091−3624 we do not have an estimation of the distance, the inclination angle, BH mass and spin, and the properties of the companion star. Some results on optical and NIR counterpart of IGR J17091−3624 have been reported by Torres et al. (2011).

Chaty et al. (2008), on the basis of optical and NIR photometric and spectroscopic studies of two possible counterparts of the source, suggested that the source should belong to the Galactic bulge. However, Rodriguez et al. (2011b) recently estimated a lower limit of the source distance from its hard to soft transition luminosity concluding that, if the transition occurred at luminosity that spans from 4 to 10 per cent of the Eddington luminosity (assuming a BH mass of 10 $M_\odot$), IGR J17091−3624 is farther from the Galactic bulge, at

---

[6] The inner disc radius values reported for GRS 1915+105 by Muno et al. (1999) and related to inner temperatures greater than 1.6 keV are too small to be associated with the ISCO for any reasonable BH mass. Even if the hard part of the spectrum, modelled using a power law, could underestimate the inner disc radius (Done et al. 2007), it is not possible to exclude that, in these cases, the accretion geometry could be different from the one predicted by MDBB. However, this should not be the case for IGR J17091−3624. In fact, the spectral parameters reported in our analysis are not as extreme as the ones reported by Muno et al. (1999) for GRS 1915+105.

a distance that spans from about 11 up to 17 kpc. Moreover, Pahari et al. (2011b), using a different method, based on QPO, estimated an even larger distance of 20 kpc and a mass range spanning from 8 to 11.4 $M_{\odot}$.

Assuming a distance range of 11–17 kpc, the bolometric luminosities of IGR J17091−3624 estimated from the observation displaying 'heartbeat' with the highest flux would be (3–7) × 10^{37} erg s^{-1}, which translates into $L \sim$ (3–6) per cent $L_{\rm Edd}$. However, considering the distance and the BH mass range supposed by Pahari et al. (2011b), these luminosities result in 1 and 8 per cent $L_{\rm Edd}$.

Since the flare-like events should be at Eddington limit regime (see e.g. Nayakshin & Rappaport 2000; Neilsen et al. 2011, and reference therein), if we consider the values reported above, we conclude that the faintness of IGR J17091−3624 should not be only due to the source distance. For this reason, Altamirano et al. (2011d) supposed that the distance of the source could be even larger than 20 kpc, otherwise the BH mass should be extremely small (less than 3 $M_{\odot}$).

Other peculiar differences between IGR J17091−3624 and GRS 1915+105 are the lack of detection of the Compton reflection component and the extremely low apparent inner disc radius (see Section 3.2).

Taking these results as a whole, we speculate that IGR J17091−3624 could be a highly inclined system and we suggest that the lower luminosity of IGR J17091−3624 could also be ascribed to the spectral deformation effects due to the high inclination angle as reported by Cunningham (1998). Indeed, when a Kerr BH is seen at a high inclination angle ($\cos i < 0.25$, $i \sim 75°$), the source appears significantly fainter (up to a factor that depends on the BH spin and mass but can reach about an order of magnitude less) with respect to the system observed face-on.

At odds with this hypothesis is the lack of detection of eclipses. Although we do not have any information about the system, such as the orbital period or the companion star mass, we can speculate that the lack of eclipses could be related to a small ratio between the companion star and the BH mass. Using the Eggleton approximation (Eggleton 1983), we calculated the relation between the mass ratio q ($M_{\rm star}/M_{\rm BH}$) and the Roche lobe radius. Then, the minimum inclination angle, i, for which the Roche lobe does not cover the central engine along the observer line of sight, is extracted from simple geometrical considerations giving

$$R_{\rm L}/a < \cos i, \tag{1}$$

where $R_{\rm L}$ is the Roche lobe radius calculated with the Eggleton approximation, a is the distance between the BH and the companion star and i is the inclination angle of the system. Plotting $R_{\rm L}/a$ versus q (Eggleton 1983) and considering equation (1), we found that for $q < 0.2$, the Roche lobe does not cover the central engine for inclination angles smaller than 75° (Cunningham 1998).

Moreover, the lack of information on the orbital period of the system hampers the search for the eventual presence of partial eclipses via the usual light-curve folding techniques that increase the signal-to-noise ratio.

5 CONCLUSIONS

The outcome of the observational campaign presented here suggests that IGR J17091−3624 can no longer be considered as a typical transient BH (Fender et al. 2004). After the transition from the hard to the soft state in 2011 (Rodriguez et al. 2011b), the source did not follow the standard q-track in the HID diagram (see e.g. Homan et al. 2001; Homan & Belloni 2005, and reference therein) and, since March 2011, it remained trapped in an oscillatory state, similar to that observed during the flaring states of GRS 1915+105 (Altamirano et al. 2011d).

As mentioned above (see Section 4.1), the pseudo-periodic bursts in the light curve of GRS 1915+105 reach the Eddington luminosity and are believed to be related to disc oscillations. The physics that drives these inner disc oscillations is connected with both the local Eddington limit and the radiation pressure instability. If the 'heartbeat' oscillations seen from IGR J17091−3624 are interpreted as being due to the same mechanism as in GRS 1915+105 (as also supposed by Altamirano et al. 2011d), then the apparent 'faintness' of IGR J17091−3624 remains unexplained unless to suppose a huge distance or an extremely low BH mass (Altamirano et al. 2011d).

In Section 4.1 we noted that a reduction of the apparent luminosity up to an order of magnitude can also be achieved if the system is seen nearly edge-on (for inclination angles <75°; Eggleton 1983). According to this idea and considering also the $L/L_{\rm Edd}$ ratio calculated for the different distance values, we can speculate that the source, probably, not only lies far from the Galactic bulge, in agreement with Rodriguez et al. (2011b), but it is also observed at a high inclination angle. As also discussed in Section 4.1, this finding is not in contrast with the lack of eclipses in the source light curve. In fact, if the companion star is small, the eclipses can be undetected even for a high inclination angle, as for example in the case of the BHC XTE J1118+480 (see e.g. McClintock et al. 2001; Wagner et al. 2001).

We note that at present we cannot exclude that the faintness of IGR J17091−3624 is only due to a very large distance (>20 kpc) or to the extremely low BH mass (<3 $M_{\odot}$), as suggested by Altamirano et al. (2011d). The large distance, unusual for low-mass X-ray binaries generally concentrated in the Galactic bulge (Grimm et al. 2002), could agree with the hypothesis reported by Jonker & Nelemans (2004) that the distances of the LMXB could be affected by a systematic error due to misclassification of the companion star.

However, recent results, reported by King et al. (2012), based on a *Chandra* observation campaign support the hypothesis that IGR J17091−3624 is observed at a high inclination angle. Future refined estimation of the distance and the BH mass of IGR J17091−3624 might help understand if GRS 1915+105 and IGR J17091−3624 are very similar objects as simply observed at very different distances or inclination angles. We point out that the high inclination of the system is a possible scenario to explain the low luminosity of the source without invoking very large distances or extremely low BH masses that may challenge the Rhoades–Ruffini limit (Rhoades & Ruffini 1974).

Finally, we suggest that, as in the case of GRS 1915+105, IGR J17091−3624 might also show a 'quasi-persistent' outburst of the order of years. Thus, the *INTEGRAL* and *Swift* observation campaign of the 2011 outburst probably caught the evolution of a transient BH in a persistent GRS 1915+105-like phase.

ACKNOWLEDGMENTS

FC, MDS, AP and GDC acknowledge financial support from the agreement ASI-INAF I/009/10/0. FC thanks Giorgio Matt and Piergiorgio Casella for useful scientific discussions. MDS and GDC acknowledge contribution by the grant PRIN-INAF 2009. We would like to thank N. Gehrels and the *Swift* Team for making *Swift* observations possible. A special thanks goes to E. Kuulkers and the *INTEGRAL* Galactic bulge monitoring programme. *INTEGRAL* is an ESA project with instruments and science data centre funded by

ESA member states especially the PI countries: Denmark, France, Germany, Italy, Switzerland, Spain, Czech Republic and Poland, and with the participation of Russia and the USA.

REFERENCES

Altamirano D. et al., 2011a, Astron. Telegram, 3225

Altamirano D. et al., 2011b, Astron. Telegram, 3230

Altamirano D. et al., 2011c, Astron. Telegram, 3299

Altamirano D. et al., 2011d, ApJ, 742, L17

Belloni T., Mendez M., King A. R., van der Klis M., van Paradijs J., 1997, ApJ, 479, L145

Belloni T., Klein-Wolt M., Mendez M., van der Klis M., van Paradijs J., 2000, A&A, 355, 271

Bozzo E., Giunta A., Stella L., Falanga M., Israel G., Campana S., 2009, A&A, 502, 21

Burrows D. et al., 2005, Space Sci. Rev., 120, 165

Capitanio F. et al., 2005, ApJ, 622, 503

Capitanio F. et al., 2009a, ApJ, 690, 1621

Capitanio F., Belloni T., Del Santo M., Ubertini P., 2009b, MNRAS, 398, 1194

Capitanio F. et al., 2011, Astron. Telegram, 3159

Chaty S., Rahoui F., Foellmi C., Tomsick J. A., Rodriguez J., Walter R., 2008, A&A, 484, 783

Corbel S., Rodriguez J., Tzioumis T., Tomsick J., 2011, Astron. Telegram, 3167

Courvoisier T. J.-L. et al., 2003, A&A, 411, 53L

Cunningham C. T., 1998, ApJ, 202, 788

Del Santo M. et al., 2011, Astron. Telegram, 3203

Devis W. D., Done C., Blaes O. M., 2006, ApJ, 647, 525

Done C., Gierlinski M., Kubota A., 2007, A&AR, 15, 1

Eggleton P. P., 1983, ApJ, 268, 368

Fender R., Belloni T., 2004, ARA&A, 42, 317

Fender R. P., Belloni T., Gallo E., 2004, MNRAS, 355, 1105

Frontera F. et al., 2001, ApJ, 561, 1006

Gierlinsky M., Zdziarski A. A., Putanen J., Coppi P. S., Ebisawa K., Johnson W. N., 1999, MNRAS, 309, 496

Grebenev S. A., Molkov S. V., Sunyaev R. A., 2005, Astron. Telegram, 444

Grimm H.-J., Gilfanov M., Suyaev R., 2002, A&A, 391, 923

Homan J., Belloni T., 2005, Ap&SS, 300, 107

Homan J., Wijnands R., van der Klis M., Belloni T., van Paradijs J., Klein-Wolt M., Fender R., Mendez M., 2001, ApJS, 132, 377

in't Zand J. J. M., Heise J., Lowes P., Ubertini P., 2003, Astron. Telegram, 160

Jonker P. G., Nelemans G., 2004, MNRAS, 354, 255

Jourdain E., Gotz D., Westergaard N. J., Natalucci L., Roques J. P., 2008, 7th INTEGRAL Workshop, Proc. Sci, 144

Kennea J. A., Capitanio F., 2009, Astron. Telegram, 1140

King A. L. et al., 2012, ApJ, 746, 20

Krimm H. A., Kennea J. A., 2011, Astron. Telegram, 3148

Krimm H. A. et al., 2011, Astron. Telegram, 3144

Kubota A., Tanaka Y., Makishima K., Ueda Y., Dotani T., Inoue H., Yamaoka K., 1998, PASJ, 50, 667

Kuulkers E., Lutovinov A., Parmar A., Capitanio F., Mowlavi N., Hermsen W., 2003, Astron. Telegram, 149

Lebrun F. et al., 2003, A&A, 411, 141

Lightman A. P., Eardley D. M., 1974, ApJ, 187, L1

Lund N. et al., 2003, A&A, 411, 231L

Lutovinov A. A., Revnivtsev M. G., 2003, Astron. Lett., 29, 719

Lutovinov A. A., Revnivtsev M., Molkov S., Sunyaev R., 2005, A&A, 430, 997

McClintock J. E., Garcia M. R., Caldwell N., Falco E. E., Garnavich P. M., Zhao P., 2001, ApJ, 551, L147

Magdziarz P., Zdziarski A. A., 1995, MNRAS, 273, 837

Martocchia A., Matt G., Karas V., Belloni T., Feroci M., 2002, A&A, 387, 215

Mineo T., Massaro E., Cusumano G., 2010, AIP Conf. Proc., 1248, 183

Mitsuda K. et al., 1984, PASJ, 36, 741

Muno M. P., Morgan E. H., Remillard R., 1999, ApJ, 527, 321

Munoz-Darias T., Motta S., Belloni T. M., 2011, MNRAS, 410, 679

Naik S., Agrawal P. C., Rao A. R., Paul B., 2002, MNRAS, 330, 487

Nayakshin S., Rappaport S., 2000, ApJ, 535, 798

Neilsen J., Remillard R. A., Lee J. C., 2011, ApJ, 737, 69

Pahari M., Yadav J. S., Bhattacharyya S., 2011a, Astron. Telegram, 3418

Pahari M., Yadav J. S., Battacharyya S., 2011b, ApJ, submitted, preprint (arXiv:1105.4694)

Pandey M., Manchanda R., Rao A. P., Durouchoux P., Ishwara-Chandra C. H., 2006, A&A, 446, 471

Remillard R. A., McClintock J. E., 2006, ARA&A, 44, 49

Revnivtsev M., Gilfanov M., Churazov E., Sunyaev R., 2003, Astron. Telegram, 150

Rhoades C., Ruffini R., 1974, Phys. Rev. Lett., 32, 324

Rodriguez J., Corbel S., Tomsick J. A., Paizis A., Kuulkers E., 2011a, Astron. Telegram, 3168

Rodriguez J., Corbel S., Caballero I., Tomsick J. A., Tzioumis T., Paizis A., Cadolle Bel M., Kuulkers E., 2011b, A&A, 533, L4

Ross R. R., Fabian A. C., 2007, MNRAS, 381, 1697

Rupen M. P., Mioduszewski A. J., Dhawan V., 2003, Astron. Telegram, 150

Shaposhnikov N., 2001, Astron. Telegram, 3179

Szuszkiewicz E., Miller J. C., 1998, MNRAS, 298, 888

Torres M. A. P., Jonker P. G., Steeghs D., Mulchaey J. S., 2011, Astron. Telegram, 3150

Ubertini P. et al., 2003, A&A, 411, 131

Wagner R. M., Foltz C. B., Shahbaz T., Casares J., Charles P. A., Starrfield S. G., Hewett P., 2001, ApJ, 556, 42

Zhang S. N., Cui W., Chen W., 1997, ApJ, 482, L155

This paper has been typeset from a TEX/LATEX file prepared by the author.